# Surface Passivation enabled by Atomic Layer Deposited Ultra-Thin Titanium Oxide for High-efficiency Organic Solar Cells

Leiping Duan[1], Borong Sang[1], Yu Zhang[1], Yingping Zou[2], Ashraf Uddin[1] and Bram Hoex[1]

*[1] School of Photovoltaic and Renewable Energy Engineering, University of New South Wales, Sydney, NSW 2052, Australia.*
*[2] College of Chemistry and Chemical Engineering, Central South University, Changsha 410083, P.R. China*

Organic solar cells (OSCs) are considered to reach its second golden age with the profoundly improved power conversion efficiency (PCE) and device stability. [1-4] OSCs do not contain toxic elements such as lead as is the case for the record efficiency perovskite solar cells. Semitransparent OSCs (ST-OSCs) also showing aesthetical advantages over other semitransparent photovoltaic installations. Originating from the diversity in organic light-absorbing materials, ST-OSCs can be fabricated in various colors.[5] To date, atomic layer deposition (ALD) metal oxide for surface passivation was widely demonstrated in silicon, dye-sensitized, perovskite, and chalcogenide thin-film solar cells to improve the device performance, while was less investigated for OSCs. [6-11] In this work, we reported for the first time the application of the ALD deposited ultrathin $TiO_2$ as the surface passivation layer in OSCs. The addition of 2 cycles of ultrathin ALD $TiO_2$ layer not only effectively passivated the interface between the ZnO electron transport layer (ETL) and the active layer, but also reduced series resistance and improved charge transport process in the device. We achieved an absolute 1% increase in PCE by using the optimized 2 cycles of ultrathin ALD $TiO_2$ layer in the device.

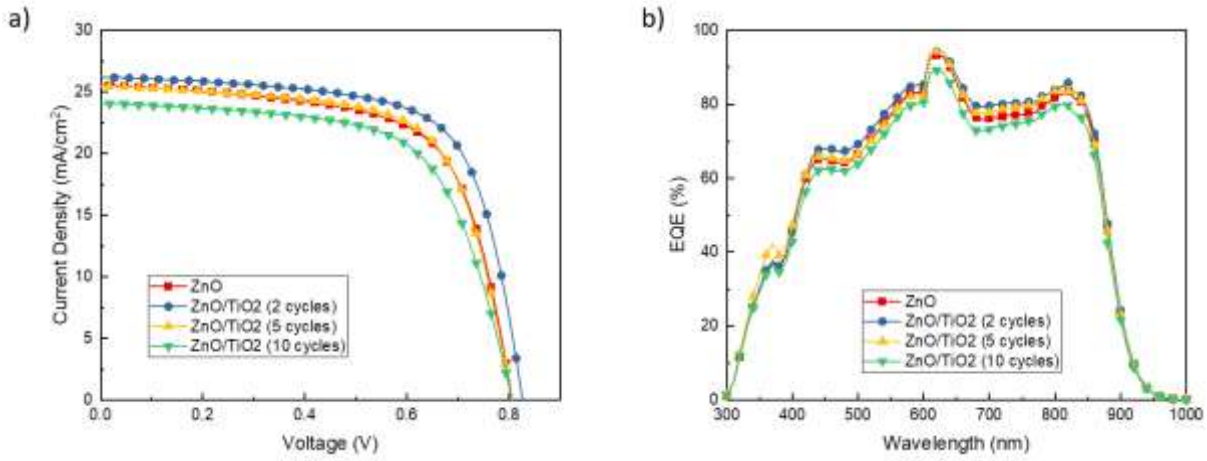


**Figure 1. a) Current density to voltage (J-V) curves and b) external quantum efficiency (EQE) spectrum of fabricated OSCs with different ALD cycles of ultrathin TiO2 layer.**

**Table I. Open circuit voltage ($V_{oc}$), short circuit current density ($J_{sc}$), fill factor (FF), power conversion efficiency (PCE), shunt resistance ($R_{sh}$) and series resistance ($R_s$) of fabricated OSCs with different ALD cycles of ultrathin TiO2 layer**

| Devices | $V_{oc}$ (V) | $J_{sc}$ ($J_{cal}$) (mA/cm$^2$) | *FF* | Ave (Best) PCE | $R_{sh}$ (Ω cm$^2$) | $R_s$ (Ω cm$^2$) |
|---|---|---|---|---|---|---|
| ZnO | 0.81±0.01 | 24.96±0.55 (24.88) | 0.67±0.01 | 13.56%±0.15% (13.79%) | 768.1±99.1 | 5.61±0.57 |

| | | | | | | |
|---|---|---|---|---|---|---|
| ZnO/TiO2 (2 cycles) | 0.81±0.01 | 25.89±0.27 (25.62) | 0.69±0.01 | 14.62%±0.23% (14.87%) | 831.1±108.1 | 4.70±0.28 |
| ZnO/TiO2 (5 cycles) | 0.81±0.00 | 25.32±0.49 (25.11) | 0.66±0.01 | 13.60%±0.34% (14.13%) | 778.1±53.1 | 6.01±0.43 |
| ZnO/TiO2 (10 cycles) | 0.81±0.00 | 23.58±0.55 (23.82) | 0.63±0.02 | 12.07%±0.27% (12.42%) | 747.1±69.1 | 7.40±1.17 |

In this study, we integrated an ultrathin ALD-$TiO_2$ layer as the surface passivation layer on top of ZnO ETL to improve the device performance of the N3 based OSCs. The thickness of the ALD-$TiO_2$ layer was optimized with different ALD cycles from 2 to 10, which corresponding to 0.1 to 0.5 nm. The current density to voltage (J-V) curves and external quantum efficiency (EQE) of fabricated devices are shown in Figure 1 (a) and (b). The corresponding photovoltaic parameters of those devices with different cycles of the ALD-$TiO_2$ layer are listed in Table I. For the device with 2 cycles of ALD-$TiO_2$, an obvious increase can be observed in the device performance. Further increase in the ALD cycles of $TiO_2$ caused decreases in the device performance. 2 ALD cycles seem to be the optimum parameter for the ultrathin $TiO_2$ layer in the device. As a result, the device with 2 cycles of ALD-$TiO_2$ layer achieved the best PCE of 14.87 % with a $V_{oc}$ of 0.81 V, $J_{sc}$ of 25.89 mA/cm$^2$ and FF of 0.69, enabling an absolute 1% enhancement in PCE compared to the control device. It was found that this enhancement in PCE has mainly come from an increase in $J_{sc}$ and FF. The increase in FF was found to result from the decreased series resistance and slightly increased shunt resistance in the device. Incorporating 2 cycles of ALD-$TiO_2$ can reduce the series resistance of the device, while further increase the ALD cycles can cause the series resistance increase. EQE spectrum of devices reveals that both devices with 2 and 5 cycles of the ALD-$TiO_2$ layer can have a higher $J_{sc}$ value than the control device, which is consistent with the *J-V* results.

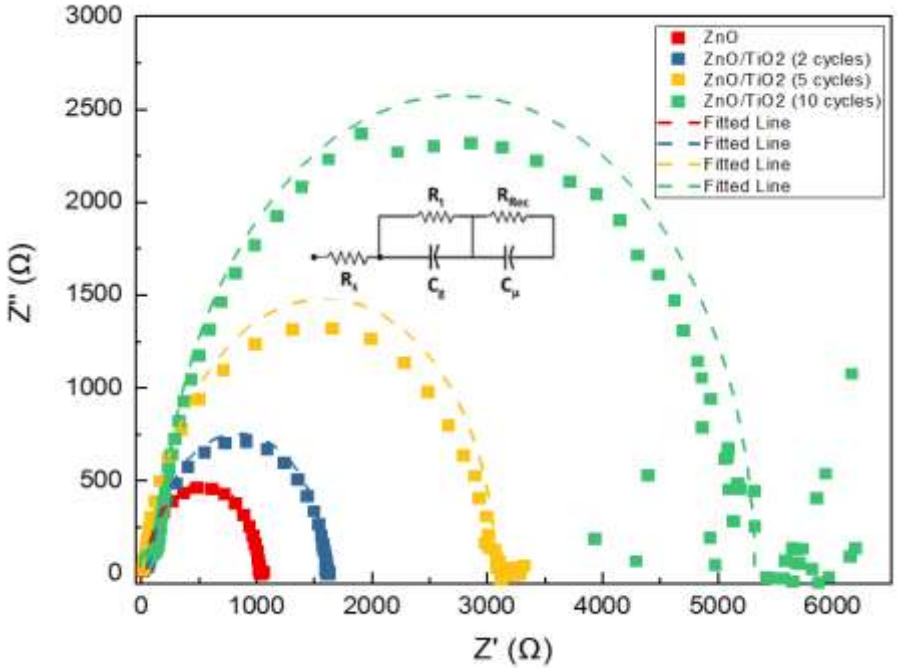


**Figure 2. Nyquist plots with the equivalent electrical circuit at a bias of 700 mV under the dark condition for fabricated OSCs with different ALD cycles of ultrathin $TiO_2$ layer.**

**Table III. Extracted $R_s$, $R_t$, $R_{rec}$, $C_g$, and $C_\mu$ value fitted from the Nyquist plot of fabricated OSCs with different ALD cycles of ultrathin $TiO^2$ layer.**

| Devices | $R_s$ ($\Omega$ cm$^2$) | $R_t$ ($\Omega$ cm$^2$) | $R_{rec}$ ($\Omega$ cm$^2$) | $C_g$ (uF/cm$^2$) | $C_u$ (uF/cm$^2$) |
|---|---|---|---|---|---|
| ZnO | 1.75 | 5.77 | 115.92 | 0.25 | 0.14 |
| ZnO/TiO2 (2 cycles) | 5.03 | 5.90 | 181.20 | 0.09 | 0.12 |
| ZnO/TiO2 (5 cycles) | 2.45 | 12.24 | 354.00 | 0.25 | 0.11 |
| ZnO/TiO2 (10 cycles) | 3.14 | 16.68 | 618.00 | 0.02 | 0.08 |

EIS was used to measure the response of the device when an external alternating current (AC) is applied.[12, 13] The applied biased voltage was set at 0.7 V for all samples, of which value is slightly lower than their $V_{oc}$.[14] Figure 2 shows the Nyquist plots from EIS results, and the curves were fitted with an equivalent electrical circuit (EEC). It is apparent tthat the $R_{rec}$ value of the device increased with increasing the ALD cycles of $TiO_2$ layer. 10 cycles of the ALD $TiO_2$ layer delivered the highest $R_{rec}$ of 618 $\Omega$ cm$^{2,}$ which is over 5 times higher than the control device. In the EIS study, $R_{rec}$ represents the ability of the device to suppress the non-radiative recombination.[15, 16] The higher $R_{rec}$ value indicates the lower non-radiative recombination in the device. Hence, the result demonstrate that the incorporation of ultrathin ALD $TiO_2$ layer can suppress the non-radiative recombination in the device. The thicker ALD $TiO_2$ layer contributed to a lower non-radiative recombination. As the active layer and HTL were identical for all devices, the suppressed non-radiative recombination is mainly resulting from a reduction in surface recombination at the interface between the active layer and ETL. Therefore, the ultrathin ALD $TiO_2$ layer was shown to provide surface passivation, where the thicker ALD $TiO_2$ layer can deliver a higher level of surface passivation. The increase in $R_t$ can suggest the impediment of interfacial charge transfer rate.[17, 18] Herein, the device with 2 cycles of ALD $TiO_2$ layer has a similar $R_t$ value when compared to the control device, which indicated that the interfacial charge transfer rate is less affected by such an ultrathin layer. However, further increasing the ALD cycles of $TiO_2$ layer caused a significant increase in $R_t$ value, which points to the decreased charge transfer rate in the device. This can be the reason why 5 and 10 cycles of ALD $TiO_2$ delivered a similar or lower device performance compared to the control device.

In summary, we optimized the ALD cycles of $TiO_2$ layer for OSCs and found that 2 cycles of ALD TiO2 layer is the optimum case. The addition of 2 cycles of ultrathin ALD $TiO_2$ layer not only can effectively passivate the interface between the ZnO electron transport layer and the active layer but also can reduce the series resistance and improve charge transport process in the device.

**References**

1. Aernouts, T., et al., *Printable anodes for flexible organic solar cell modules.* Thin Solid Films, 2004. **451-452**: p. 22-25.

2. Duan, L., et al., *Progress in non-fullerene acceptor based organic solar cells.* Solar Energy Materials and Solar Cells, 2019. **193**: p. 22-65.
3. Kaltenbrunner, M., et al., *Ultrathin and lightweight organic solar cells with high flexibility.* Nature Communications, 2012. **3**(1): p. 770.
4. Khalil, A., et al. *Review on organic solar cells*. in *2016 13th International Multi-Conference on Systems, Signals & Devices (SSD)*. 2016.
5. Shin, D.H. and S.-H.J.C. Choi, *Recent studies of semitransparent solar cells.* 2018. **8**(10): p. 329.
6. Lin, C., et al., *Enhanced performance of dye-sensitized solar cells by an Al2O3 charge-recombination barrier formed by low-temperature atomic layer deposition.* Journal of Materials Chemistry, 2009. **19**(19): p. 2999-3003.
7. Brennan, T.P., et al., *The importance of dye chemistry and TiCl4 surface treatment in the behavior of Al2O3 recombination barrier layers deposited by atomic layer deposition in solid-state dye-sensitized solar cells.* Physical Chemistry Chemical Physics, 2012. **14**(35): p. 12130-12140.
8. Koushik, D., et al., *High-efficiency humidity-stable planar perovskite solar cells based on atomic layer architecture.* Energy & Environmental Science, 2017. **10**(1): p. 91-100.
9. Hsu, W.-W., et al., *Surface passivation of Cu(In,Ga)Se2 using atomic layer deposited Al2O3.* 2012. **100**(2): p. 023508.
10. Kim, J., et al., *Improving the open-circuit voltage of Cu2ZnSnSe4 thin film solar cells via interface passivation.* 2017. **25**(4): p. 308-317.
11. Cui, X., et al., *Cd-Free Cu2ZnSnS4 solar cell with an efficiency greater than 10% enabled by Al2O3 passivation layers.* Energy & Environmental Science, 2019. **12**(9): p. 2751-2764.
12. Garcia-Belmonte, G., A. Guerrero, and J. Bisquert, *Elucidating Operating Modes of Bulk-Heterojunction Solar Cells from Impedance Spectroscopy Analysis.* The Journal of Physical Chemistry Letters, 2013. **4**(6): p. 877-886.
13. Haque, F., et al., *Effects of Hydroiodic Acid Concentration on the Properties of CsPbI3 Perovskite Solar Cells.* ACS Omega, 2018. **3**(9): p. 11937-11944.
14. Haque, F., et al., *Optimisation of annealing temperature for low temperature processed inverted structure Caesium Formamidinium Lead Triiodide perovskite solar cells.* Materials Science in Semiconductor Processing, 2019. **102**: p. 104580.
15. Arredondo, B., et al., *Monitoring degradation mechanisms in PTB7:PC71BM photovoltaic cells by means of impedance spectroscopy.* Solar Energy Materials and Solar Cells, 2016. **144**: p. 422-428.
16. Duan, L., et al., *Relationship Between the Diode Ideality Factor and the Carrier Recombination Resistance in Organic Solar Cells.* IEEE Journal of Photovoltaics, 2018. **8**(6): p. 1701-1709.
17. Upama, M.B., et al., *Organic solar cells with near 100% efficiency retention after initial burn-in loss and photo-degradation.* Thin Solid Films, 2017. **636**: p. 127-136.
18. Upama, M.B., et al., *Effect of annealing dependent blend morphology and dielectric properties on the performance and stability of non-fullerene organic solar cells.* Solar Energy Materials and Solar Cells, 2018. **176**: p. 109-118.